Title

Intra- and Interfractional Variations in Geometric Arrangement between Lung Tumours and Implanted Markers

Authors

Nami Ueki, M.D.,[1] Yukinori Matsuo, M.D., Ph.D.,[1] Mitsuhiro Nakamura, Ph.D.,[1] Nobutaka Mukumoto, M.S.,[1] Yusuke Iizuka, M.D.,[1] Yuki Miyabe, M.S.,[1] Akira Sawada, Ph.D.,[2] Takashi Mizowaki, M.D., Ph.D.,[1] Masaki Kokubo, M.D., Ph.D,[3] and Masahiro Hiraoka, M.D., Ph.D.[1]

Affiliation

[1] Department of Radiation Oncology and Image-applied Therapy, Kyoto University Graduate School of Medicine, Kyoto, Japan.

[2] Faculty of medical science, Kyoto College of Medical Science, Nantan, Japan.

[3] Department of Radiation Oncology, Kobe City Medical Center General Hospital, Kobe, Japan

Corresponding author

Yukinori Matsuo, M.D., Ph.D., Department of Radiation Oncology and Image-applied Therapy, Graduate School of Medicine, Kyoto University,

Phone: +81-75-751-3762, fax: +81-75-771-9749

E-mail: ymatsuo@kuhp.kyoto-u.ac.jp

Running header

Variation between lung tumour and markers

Keywords

Lung cancer, fiducial marker, positional variation, 4DCT.

Number of pages: 17

Number of tables and figures: 5

Abstract

Purpose: To quantify the intra- and interfractional variations between lung tumours and implanted markers.

Materials and Methods: Gold markers were implanted transbronchially around a lung tumour in fifteen patients. They underwent four-dimensional computed tomography scans twice, and the centroids of the tumour and markers were determined. Intrafractional variations were defined as the residual tumour motions relative to the markers due to respiration from the end-exhale phase. Interfractional variations were defined as the residual setup errors after correction for the position of the implanted markers in end-exhale phase images.

Results: The intrafractional variations differed between patients. The root mean squares of standard deviations for each phase were 0.6, 0.9, and 1.5 mm in the right-left, anterior-posterior, and superior-inferior directions, respectively. The maximum difference in intrafractional variation among 10 phases was correlated with the amplitude of tumour motion in all directions and the tumour-marker distance in the anterior-posterior and superior-inferior directions. The interfractional variations were within 2.5 mm.

Conclusions: The intrafractional variations differed according to the amount of tumour motion and the tumour-marker distance. Additionally, interfractional variations of up to 2.5 mm were observed. Thus, a corresponding margin should be considered during implanted marker-based beam delivery to account for these variations.

Introduction

Stereotactic body radiation therapy (SBRT) is an innovative technique that delivers high-dose radiation limited precisely to the region of the tumour [1,2]. In SBRT for targets affected by respiratory motion, such as lung tumours, appropriate motion management is recommended to reduce doses delivered to the surrounding normal tissues. Several methods of accounting for respiratory motion have been developed, including methods in which the radiation delivery is synchronised with respiration; *i.e*. the dynamic tumour tracking (DTT) method and the respiratory gating method [3].

With the above respiratory-synchronised methods, markers implanted either in the tumour itself or nearby are often used as the internal surrogate to localise the tumour position [4-6]. However, the position of the implanted markers does not always represent the tumour position because the tumour and markers move non-synchronously during respiration, especially in cases in which the markers were located slightly distal from the tumour [7]. This intrafractional positional difference between the tumour and markers should be incorporated into the DTT or respiratory gating irradiation treatment plan by using a wider gating window, within which the beam is delivered during the respiration cycle. Furthermore, the relative position of the tumour with respect to the markers may vary from day to day; therefore, the interfractional positional difference must be addressed. However, little about these variations is known.

The purpose of this study was to quantify the intra- and interfractional variations between the lung tumour position and the position of the implanted markers to evaluate the margin necessary to account for the associated errors during respiratory-synchronised irradiation treatment.

Materials and Methods

Patients and implanted markers

Fifteen patients who underwent SBRT for a solitary lung tumour were enrolled in this study. With the approval of the Institutional Review Board, written informed consent was obtained from all patients. One to two weeks prior to the date of the computed tomography (CT) simulation, four or five disposable gold markers (Olympus Corporation, Tokyo, Japan), spherical markers with a diameter of 1.5 mm, were implanted transbronchially. The insertion technique was similar to the one reported by Harada *et al* [4]. Prior to the implantation, the relative position between tumour and bronchi was evaluated on the multiplanar reformatted CT images. The markers were implanted into the peripheral surrounding bronchi near tumour under fluoroscopy guidance. A total of 66 markers were placed. The median interval between marker placement and the CT simulation was 8 (range, 2 to 16) days. Twelve markers were coughed up before CT simulation. After CT simulation, 2 markers were coughed up on the seventh and thirteenth day, and 1 marker migrated on the sixth day after insertion. The markers that coughed up or migrated after CT simulation during the treatment period were excluded from this analysis. No adverse effect associated with the implantation was observed. The characteristics of patients and tumours are shown in Table 1.

Patient set-up and four-dimensional CT data acquisition

The patients were immobilised using vacuum immobilisation devices: BodyFix system (Elekta AB, Stockholm, Sweden) or Esform (Engineering System, Nagano, Japan). After set-up with skin marks, four-dimensional CT (4DCT) data were acquired using a 16-multidetector row CT: LightSpeed RT or BrightSpeed (General Electric Healthcare, Waukesha, WI, USA) with an axial slice thickness of 2.5 mm. The cine duration time of the scan at each couch position was set to 6.0 or 7.0 s, which was more than the maximum

observed respiratory period. Simultaneously, the respiratory phase was monitored using the Varian Real-time Position Management system (Varian Medical Systems, Palo Alto, CA, USA) under free breathing without coaching. CT slices and respiratory phase data were transferred to the Advantage SIM workstation (General Electric Healthcare, Waukesha, WI, USA) and sorted into 10 respiratory phase bins. Motion phases were assigned for each respiratory phase as percentages; end-inhalation corresponded to 0% and end-exhalation to 50%. 4DCT scans were performed during the CT simulation (CT-1) and repeated once during the course of treatment (CT-2). Fifteen pairs, corresponding to a total of thirty 4DCT scans, were obtained. The median period from the day of CT-1 until the day of CT-2 was 8 days (range, 4 to 12). All 4DCT datasets were imported into a commercial radiotherapy planning system, iPlan 4.5.1 (BrainLAB AG, Fieldkirchen, Germany).

Analysis

The intrafractional variations assessed in this study were defined as the residual tumour motions relative to the markers due to respiration. In all 10 phases of the CT-1 scans, gross tumours and implanted markers were contoured manually with a pulmonary window setting (window level, -700 Hounsfield units; window width, 2000 Hounsfield units) by a single radiation oncologist. The centroid of the tumour $G_{t,n} = (x_{t,n}, y_{t,n}, z_{t,n})$ and the centroids of all 3 to 5 markers $G_{m,n} = (x_{m,n}, y_{m,n}, z_{m,n})$ were recorded at n% respiratory phase ($0 \leq n \leq 90$). The coordinates (x, y, z) correspond to the right-left (RL), anterior-posterior (AP), and superior-inferior (SI) directions, respectively. Along each axis, a positive value corresponds to the right, anterior, and superior directions. The relative position of the tumour and centroid of markers for each phase was represented by the vector $V_n = G_{t,n} - G_{m,n}$. Using the relative positions on 50% phase images (V_{50}) as a reference, the error $E_n = V_n - V_{50}$ was calculated. The mean (M_n) and standard deviation (SD_n) of E_n in fifteen 4DCT CT-1 datasets were also

calculated. The mean and SD of M_n ($0 \leq n \leq 90$) were calculated to evaluate systematic displacement between respiratory phases. The root mean square (RMS) of SD_n ($0 \leq n \leq 90$) was calculated to evaluate interpatient variations. The range of intrafractional variations is defined as the maximum difference in E_n among 10 phases for each direction. To evaluate the influence of the tumour motion amplitude and the tumour-marker distance on the ranges of intrafractional variations, a multiple linear regression analysis was performed. The tumour motion amplitude was defined as the maximal difference in the tumour centroid position among the 10 respiratory phases in each direction. The tumour-marker distance in each direction was defined as the distance between the tumour centroid and the centroid of all 3 to 5 markers in the 50% phase images.

The interfractional variations in this study represent the residual setup errors after correction based on the implanted markers. Firstly, to correct the rotational set up errors, the 50% phase images for CT-2 were rigidly registered to the 50% phase images of CT-1 based on bony structure. Then the translational errors were modified by registering those images based on the marker centroids. The interfractional variations were evaluated as the residual difference in the tumour centroids for each direction between CT-1 and CT-2 for each patient.

Results

Tumour motion amplitude and tumour-marker distance

The median (range) tumour motion amplitudes in CT-1 were 1.8 mm (0.4 to 5.6), 3.1 mm (0.6 to 7.8), and 8.2 mm (0.9 to 28.9) in the RL, AP, and SI directions, respectively. The median values (range) of the distance between the tumour centroid and the centroid of all markers in the 50% phase images for CT-1 were 11.9 mm (1.9 to 30.5), 8.1 mm (0.7 to 35.3), and 10.3 mm (0.3 to 30.1) in the RL, AP, and SI directions, respectively.

Intrafractional variations

The divergence in the range of intrafractional variations between patients is shown in Fig. 1, and the values of E_n in the respiratory phases ($0 \leq n \leq 90$) are shown in Fig. 2. The means ± SD of M_n ($0 \leq n \leq 90$) were 0.1±0.1 mm, 0.3±0.2 mm, and 0.0±0.2 mm, and the RMS of SD_n were 0.6 mm, 0.9 mm, and 1.5 mm in the RL, AP, and SI directions, respectively. These results indicate that the systematic difference between respiratory phases is negligible. In addition, as shown in Fig. 2, the further towards inhale then the greater the intrafractional variations.

The tumour motion amplitude was positively correlated with the range of intrafractional variations in all directions, and the tumour-marker distances were also positively correlated in the AP and SI directions (Table 2).

Interfractional variations

The median (range) interfractional variations were -0.1 mm (-2.4 to 0.7), 0.1 mm (-2.3 to 2.4), and -0.6 mm (-1.3 to 1.6) in the RL, AP, and SI directions, respectively. As shown in Fig. 3, all interfractional variations were within 2.5 mm; the greatest variations were in the AP direction. The 95^{th} percentiles of interfractional variations for one side of each direction were 0.6 and 2.1 mm to the right and left, 1.9 and 2.1 mm in the anterior and posterior directions, and 1.6 and 1.3 mm in the superior and inferior directions.

Discussion

Implanted markers are often used as a surrogate for the tumour position in radiation therapy for lung tumours. The transcutaneous and transbronchial approaches are the two major methods for implantation of markers in the vicinity of lung tumours [8-13]. These procedures may cause pneumothorax as a complication, which can delay radiation delivery and could be life-threatening for those with comorbidities. The incidences of all pneumothorax and of those

179 requiring chest tube placement after transcutaneous implantation have been reported to be 30
180 to 67% and 16 to 40%, respectively [8-10]. By contrast, the reported incidence of
181 pneumothorax with the transbronchial approach is low [10-13] and in our series no
182 complication was observed. Therefore, the transbronchial approach is preferable due to its
183 less invasive nature. However, the placement of markers near or inside the tumour is more
184 difficult with the transbronchial approach than with the transcutaneous approach, because in
185 the former the markers are placed along the small bronchi near a tumour. The greater distance
186 between the tumour and markers leads to a larger positional error [14]. This error must be
187 considered when performing radiotherapy using markers placed outside the tumour. In the
188 current study, we quantified the intra- and interfractional positional variations between the
189 lung tumour and implanted markers using 4DCT scans to determine the necessary margin for
190 respiratory-synchronised irradiation using implanted markers. Another issue about the
191 markers implanted transbronchially is the low fixation rate. In our series, the fixation rate of
192 implanted markers was 77.3%: 51 of 66 markers implanted markers were fixed throughout
193 treatment. This is comparable to the reported fixation rate using the same insertion technique
194 [11]. Due to the low fixation rate, we inserted 4 or 5 markers to avoid an additional insertion
195 procedure and used multiple markers as a surrogate for the tumour position to address the
196 change in geometric arrangement of markers by dislocation.

197 Although several authors reported the intrafractional verification of the tumour position
198 by the kilo-voltage (kV) X-ray images during gating irradiation, they calculated the tumour
199 positions from the detected positions of the implanted markers assuming the relative position
200 between the tumour and markers were constant [7,15]. The planar kV X-ray imaging is
201 superior to CT in terms of the temporal resolution but it is difficult to quantify the motion of
202 tumor itself accurately on the projected images. To quantify the variations between the tumour
203 and implanted markers, we used 4DCT. Two studies are available which evaluated the

geometrical difference between tumour and markers due to respiration using 4DCT. Smith *et al*. analysed the motion of lung tissue in 10 patients with deformable registration between exhalation and inhalation of 4DCT scans and reported stronger correlations between tumour and surrounding lung tissues in the upper lobes than in the lower lobes [16]. Finally, they concluded that the correlation between the tumour and the surrounding tissue was highly specific to the patient and lobe [16]. Since the amplitude of the tumour motion is typically smaller in the upper lobe than that in the lower lobe, then it is likely the bigger variations observed in lower lobe tumours by Smith *et al*. may be related to the amplitude of motion. Yamazaki *et al*. evaluated the distances between tumours and the distal bronchi during respiration cycle with 4DCT for 8 patients. They showed that the distances in the mid-inhale to end-inhale phase images were significantly larger than the distances in the end-exhale phase images [17]. Smith *et al*. and Yamazaki *et al*. suggested that markers that are closer to the tumour give a more accurate representation of tumour motion [16,17]. These results are consistent with our findings: the values needed to compensate for the intrafractional variations differed between patients, and depended on the amplitude of tumour motion and the tumour-marker distance.

Moreover, our results indicated that the intrafractional errors were different for each patient both in direction and in amplitude, as shown in Fig 1. A uniform isotropic margin was not adequate to cover the errors observed. Consequently, the variations must be evaluated on a per-patient basis and compensated for by addition of a patient-specific margin in DTT or gating irradiation treatment with a wider gating window. In our treatment planning process of DTT, we create an enlarged target volume which cover the intrafractional variations in the following steps. Firstly, 4DCT images from each phase are translated based on the centroid of the markers. Then, the phase images are superimposed onto the 50% phase image that is used as a reference image set. Finally, the enlarged target volume is delineated encompassing gross

tumour volumes on all fused phase image. This enlarged volume can compensate for the patient-specific intrafractional variations.

All interfractional variations in the present study were within 2.5 mm. Previous reports on interfractional variations between lung tumours and implanted markers are summarised in Supplementary Table 1 (Electronic Appendix). The reported values are larger than those in this study. This discrepancy may be attributed to two causes. One is a change in tumour-marker distance during the course of treatment. Several investigators reported tumour shrinkage and deformation after radiotherapy with conventional fractionation [5,10,14], which altered the distance. Meanwhile, Imura *et al*. [11] evaluated the interfractional variations in the distances between markers using orthogonal X-ray images with a median treatment time of 6 days, and showed that the variations during treatment were within 2 mm in 95% of cases. Their results support our finding that the interfractional variation between the tumour and markers was smaller in those undergoing hypofractionated treatment than in those undergoing conventional fractionation. A second interesting finding was the respiratory phase reproducibility. Van der Voort van Zyp *et al*. assessed marker displacement compared to the centroid of the tumour in patients that underwent SBRT; however, their results were influenced by the nonsynchronous tumour-marker motion due to divergence in the timing of breath holding [6]. Persson *et al*. also used the breath-hold CT with voluntary deep inspiration [18]. The interfractional variations in the current study were evaluated using end-exhale phase images under free breathing, which has high reproducibility compared with breath-holding.

Several limitations of our study should be mentioned. Firstly, the intrafractional variations evaluated with 4DCT during a few respiration cycles may not be representative of those during treatment in some patients although a single 4DCT is thought to be reliable for the tumour motion in the majority of patients [19]. Therefore, in our institution, we validate margins to compensate for the intrafractional variations, by visual verification with kV x-ray

fluoroscopy after the margins are determined based on the simulation 4DCT. Secondly, motion artefacts affected the contouring of tumours and implanted markers evaluated in binned 4DCT images. Because of this uncertainty in contouring, the intrafractional variations for tumours with larger motion may be over- or underestimated [20]. Furthermore, we evaluated the position of markers of 1.5-mm diameter using 4DCT with a 2.5-mm axial slice thickness. The use of 2.5-mm CT slice thickness would affect the accuracy of contouring the markers, with a maximum uncertainty of localising tumours and markers of 1.25 mm in the SI direction [6]. Those errors could be reduced by acquiring CT images with a thinner axial slice thickness or by the volumetric acquisition [21,22].

Conclusions

Intrafractional variations of the difference between tumour centroid and marker centroid position increased with both tumour motion amplitude and tumour-marker distance. Additionally interfractional variations of the distance between between tumour centroid and marker centroid position were observed up to 2.5mm. Thus, an appropriate margin to account for these variations should be considered when planning implanted-marker-based beam delivery.

References

[1] Blomgren H, Lax I, Naslund I, Svanstrom R. Stereotactic high dose fraction radiation therapy of extracranial tumors using an accelerator. Clinical experience of the first thirty-one patients. Acta Oncol 1995;34:861-70.

[2] Uematsu M, Shioda A, Tahara K et al. Focal, high dose, and fractionated modified stereotactic radiation therapy for lung carcinoma patients: a preliminary experience. Cancer 1998;82:1062-70.

[3] Keall PJ, Mageras GS, Balter JM et al. The management of respiratory motion in radiation oncology report of AAPM Task Group 76. Med Phys 2006;33:3874-900.

[4] Harada T, Shirato H, Ogura S et al. Real-time tumor-tracking radiation therapy for lung carcinoma by the aid of insertion of a gold marker using bronchofiberscopy. Cancer 2002;95:1720-27.

[5] Nelson C, Balter P, Morice RC et al. Evaluation of Tumor Position and PTV Margins Using Image Guidance and Respiratory Gating. Int J Radiat Oncol Biol Phys 2010;76:1578-85.

[6] van der Voort van Zyp NC, Hoogeman MS, van de Water S et al. Stability of markers used for real-time tumor tracking after percutaneous intrapulmonary placement. Int J Radiat Oncol Biol Phys 2011;81:e75-81.

[7] Seppenwoolde Y, Shirato H, Kitamura K et al. Precise and real-time measurement of 3D tumor motion in lung due to breathing and heartbeat, measured during radiotherapy. Int J Radiat Oncol Biol Phys 2002;53:822-34.

[8] Kothary N, Heit JJ, Louie JD et al. Safety and Efficacy of Percutaneous Fiducial Marker Implantation for Image-guided Radiation Therapy. J Vasc Interv Radiol 2009;20:235-39.

296 [9] Bhagat N, Fidelman N, Durack JC et al. Complications associated with the
297 percutaneous insertion of fiducial markers in the thorax. Cardiovasc Intervent Radiol
298 2010;33:1186-91.
299 [10] Kupelian PA, Forbes A, Willoughby TR et al. Implantation and Stability of Metallic
300 Fiducials Within Pulmonary Lesions. Int J Radiat Oncol Biol Phys 2007;69:777-85.
301 [11] Imura M, Yamazaki K, Shirato H et al. Insertion and fixation of fiducial markers for
302 setup and tracking of lung tumors in radiotherapy. Int J Radiat Oncol Biol Phys
303 2005;63:1442-47.
304 [12] Schroeder C, Hejal R, Linden PA. Coil spring fiducial markers placed safely using
305 navigation bronchoscopy in inoperable patients allows accurate delivery of
306 CyberKnife stereotactic radiosurgery. J Thorac Cardiovasc Surg 2010;140:1137-42.
307 [13] Harley DP, Krimsky WS, Sarkar S, Highfield D, Aygun C, Gurses B. Fiducial Marker
308 Placement Using Endobronchial Ultrasound and Navigational Bronchoscopy for
309 Stereotactic Radiosurgery: An Alternative Strategy. Ann Thorac Surg 2010;89:368-74.
310 [14] Roman NO, Shepherd W, Mukhopadhyay N, Hugo GD, Weiss E. Interfractional
311 positional variability of fiducial markers and primary tumors in locally advanced
312 non-small-cell lung cancer during audiovisual biofeedback radiotherapy. Int J Radiat
313 Oncol Biol Phys 2012;83:1566-72.
314 [15] Li R, Mok E, Chang DT et al. Intrafraction verification of gated RapidArc by using
315 beam-level kilovoltage X-ray images. Int J Radiat Oncol Biol Phys 2012;83:e709-15.
316 [16] Smith RL, Yang D, Lee A, Mayse ML, Low DA, Parikh PJ. The correlation of tissue
317 motion within the lung: Implications on fiducial based treatments. Med Phys
318 2011;38:5992-97.

[17] Yamazaki R, Nishioka S, Date H, Shirato H, Koike T, Nishioka T. Investigation of the change in marker geometry during respiration motion: a preliminary study for dynamic-multi-leaf real-time tumor tracking. Radiat Oncol 2012;7:218.

[18] Persson GF, Josipovic M, Von der Recke P et al. Stability of percutaneously implanted markers for lung stereotactic radiotherapy. J Appl Clin Med Phys 2013;14:187-95.

[19] Guckenberger M, Wilbert J, Meyer J, Baier K, Richter A, Flentje M. Is a single respiratory correlated 4D-CT study sufficient for evaluation of breathing motion? Int J Radiat Oncol Biol Phys 2007;67:1352-59.

[20] Persson GF, Nygaard DE, Brink C et al. Deviations in delineated GTV caused by artefacts in 4DCT. Radiother Oncol 2010;96:61-66.

[21] Yamashita H, Kida S, Sakumi A et al. Four-dimensional measurement of the displacement of internal fiducial markers during 320-multislice computed tomography scanning of thoracic esophageal cancer. Int J Radiat Oncol Biol Phys 2011;79:588-95.

[22] Yamashita H, Okuma K, Tada K et al. Four-dimensional measurement of the displacement of internal fiducial and skin markers during 320-multislice computed tomography scanning of breast cancer. Int J Radiat Oncol Biol Phys 2012;84:331-35.

Acknowledgments

This research was supported by the Japan Society for the Promotion of Science (JSPS) through the “Funding Program for World-leading Innovative R&D on Science and Technology” (FIRST Program).

Conflicts of interest

Takashi Mizowaki, Masaki Kokubo, and Masahiro Hiraoka have a consultancy agreement with Mitsubishi Heavy Industries, Ltd., Japan.

Figure legends

Fig. 1. The range of intrafractional variations in the RL (a), AP (b), and SI (c) directions for each patient rearranged according to the three-dimensional tumour motion amplitude in descending order. *Abbreviations*: RL, right-left; AP, anterior-posterior; SI, superior-inferior

Fig. 2. E_n values in the RL (a), AP (b), and SI (c) directions for each respiratory phase. E_n is the error in the relative position of the tumour to the centroid of the markers on n% phase images ($0 \leq n \leq 90$), using the relative position on the 50% phase images as a reference. Other abbreviations are as in Fig. 1.

Fig. 3. Interfractional variation in the RL, AP, and SI directions. Abbreviations are as in Fig. 1.

Table 1. Characteristics of patients and tumours (n=15).

Characteristics	*n* = 15
Age (y)	
Median	82
[range]	[54–87]
Gender	
Male	12
Female	3
Tumour size	
≤20 mm	4
>20 to ≤30 mm	6
>30 to ≤50mm	5
Tumour location	
Right middle lobe	2
Right lower lobe	7
Left upper lobe	2
Left lower lobe	4
No. of implanted markers	
4	9

5	6
No. of markers evaluated	
3	10
4	4
5	1

Table 2. Predictive factors for the range of intrafractional variation as determined by multiple linear regression analysis.

Predictive factor	Range of intrafractional variation					
	RL		AP		SI	
	β	*p*	β	*p*	β	*p*
Tumour motion amplitude	0.539	0.048	0.428	0.076	0.591	0.011
Tumour–marker distance	-0.051	0.84	0.449	0.064	0.327	0.012
R	0.549		0.649		0.780	

Abbreviations: R, correlation coefficient; other abbreviations are as in Fig. 1.

Supplementary Table 1. Summary of reports of interfractional variation between tumours and markers.

Author	*n*	Modality	Implanted Markers			Result
			n	Shape	Insertion	
Nelson *et al*. [5]	5	4DCT	1 to 4	Cylinder	Transbronchial	6 ± 3 mm*
Roman *et al*. [14]	7	4D CBCT	2 to 4	Long coil	Transbronchial	4 ± 2 mm (lateral), 3 ± 2 mm (AP), and 4 ± 3 mm (SI) *
Kupelian *et al*. [10]	23	Breath-hold CT (exhale)	NA	Long coil	Transcutaneous / Transbronchial	2.6 ± 1.3 mm* (range, 0.2 to 5.4)
Van der Voort van Zyp *et al*. [6]	42	Breath-hold CT (exhale)	3	Cylinder	Transcutaneous	Median 1.3 mm (range, 0.1 to 53.6)
Persson *et al.* [18]	14	Breath-hold CT (inhale)	1	Long coil	Transcutaneous	Range: -2.9 to 2.6 mm (LR), -1.8 to 1.5 mm (AP), and -2.6 to 2.8 mm (SI)
This study	15	4DCT (50%)	3 to 5	Sphere	Transbronchial	All values in each direction were within 2.5 mm

* mean ± standard deviation.

Abbreviations: 4D, four-dimensional; CT, computed tomography; CBCT, cone-beam CT; RL, right-left; AP, anterior-posterior; SI, superior-inferior

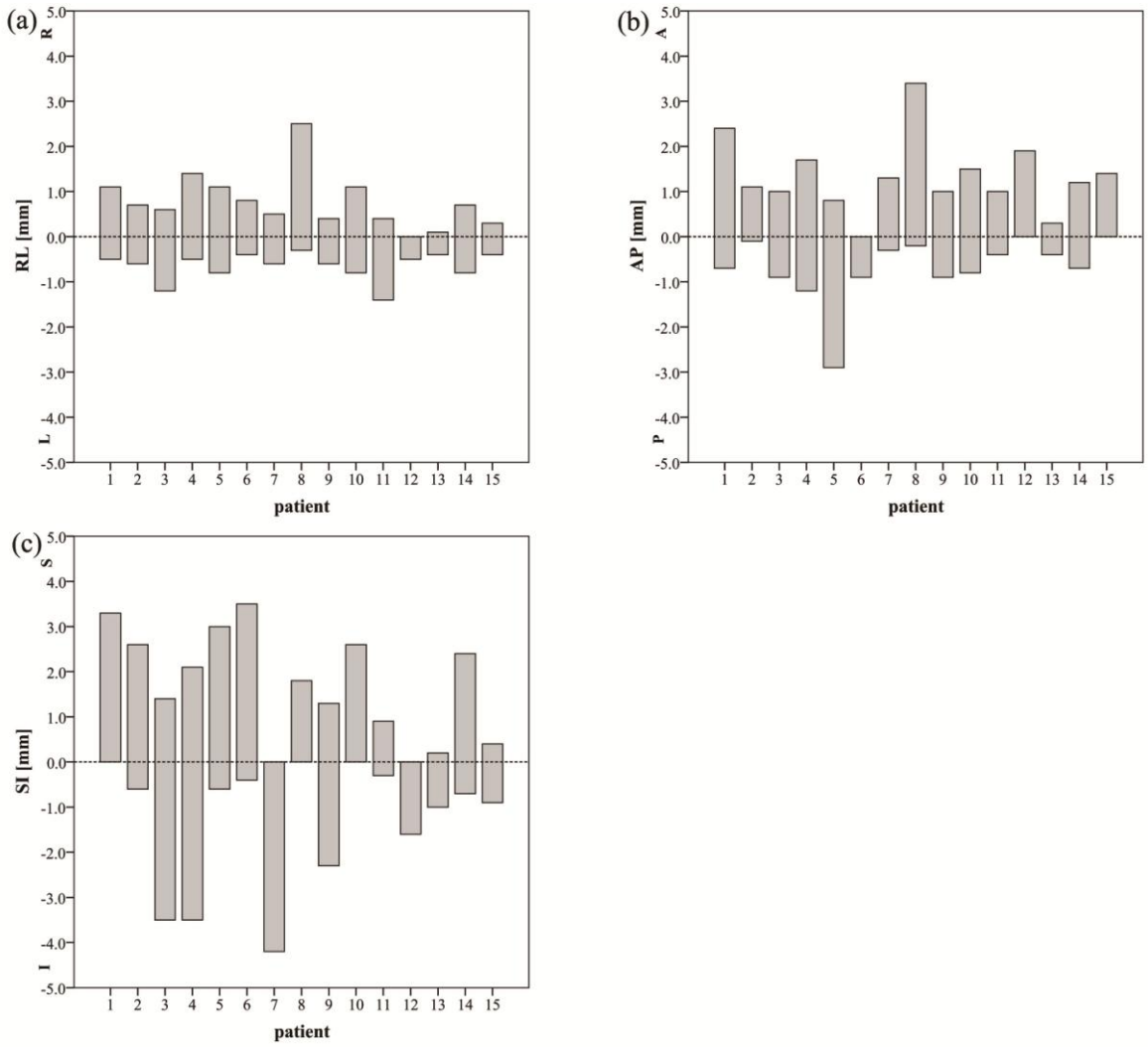
(a)
R
L
RL [mm]
5.0
4.0
3.0
2.0
1.0
0.0
-1.0
-2.0
-3.0
-4.0
-5.0
1 2 3 4 5 6 7 8 9 10 11 12 13 14 15
patient
(b)
A
P
AP [mm]
5.0
4.0
3.0
2.0
1.0
0.0
-1.0
-2.0
-3.0
-4.0
-5.0
1 2 3 4 5 6 7 8 9 10 11 12 13 14 15
patient
(c)
S
I
SI [mm]
5.0
4.0
3.0
2.0
1.0
0.0
-1.0
-2.0
-3.0
-4.0
-5.0
1 2 3 4 5 6 7 8 9 10 11 12 13 14 15
patient

Fig. 1.

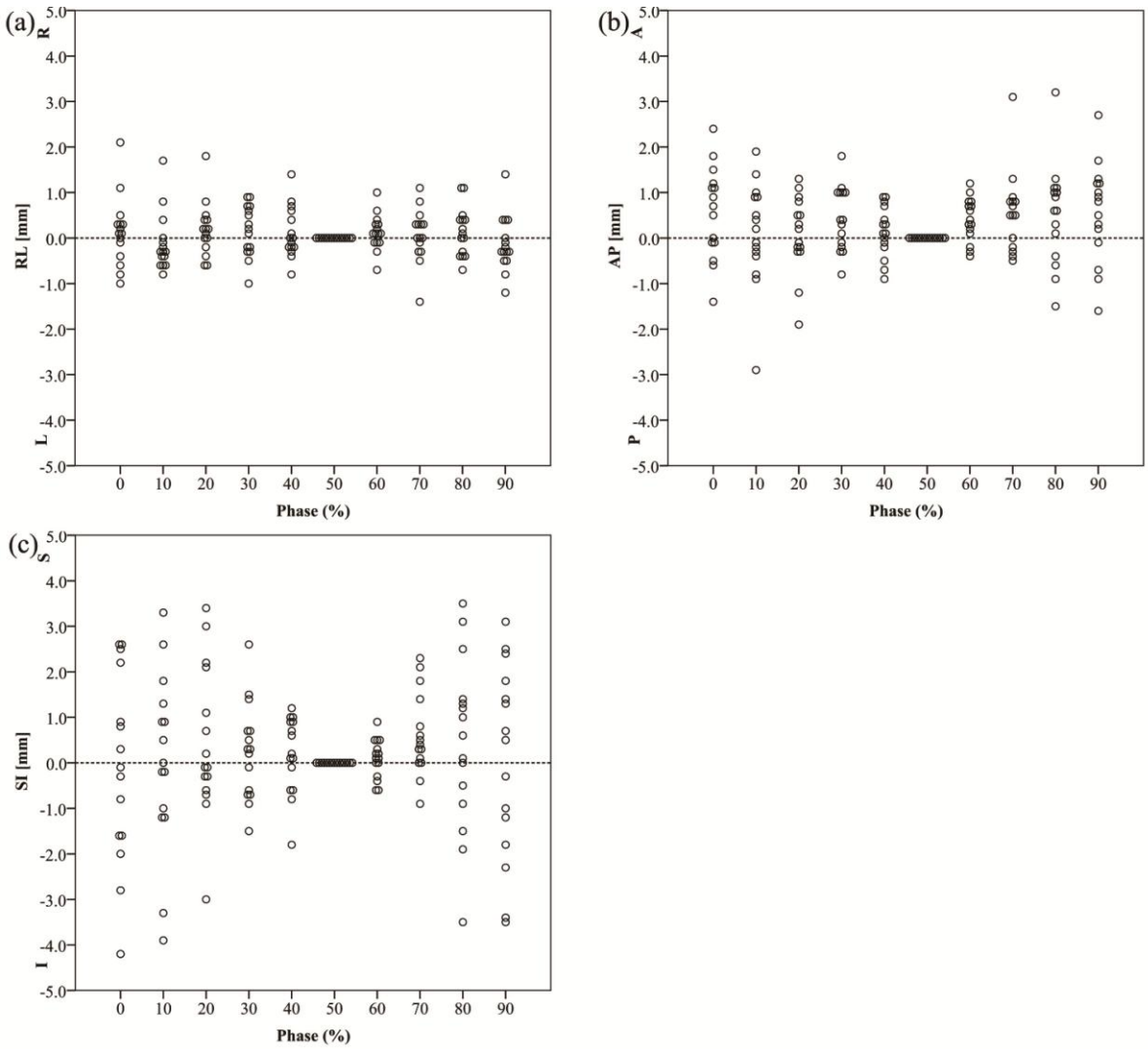
(a)
R
L
RL [mm]
5.0
4.0
3.0
2.0
1.0
0.0
-1.0
-2.0
-3.0
-4.0
-5.0
0
10
20
30
40
50
60
70
80
90
Phase (%)
(b)
A
P
AP [mm]
Phase (%)
(c)
S
I
SI [mm]
Phase (%)

Fig. 2.

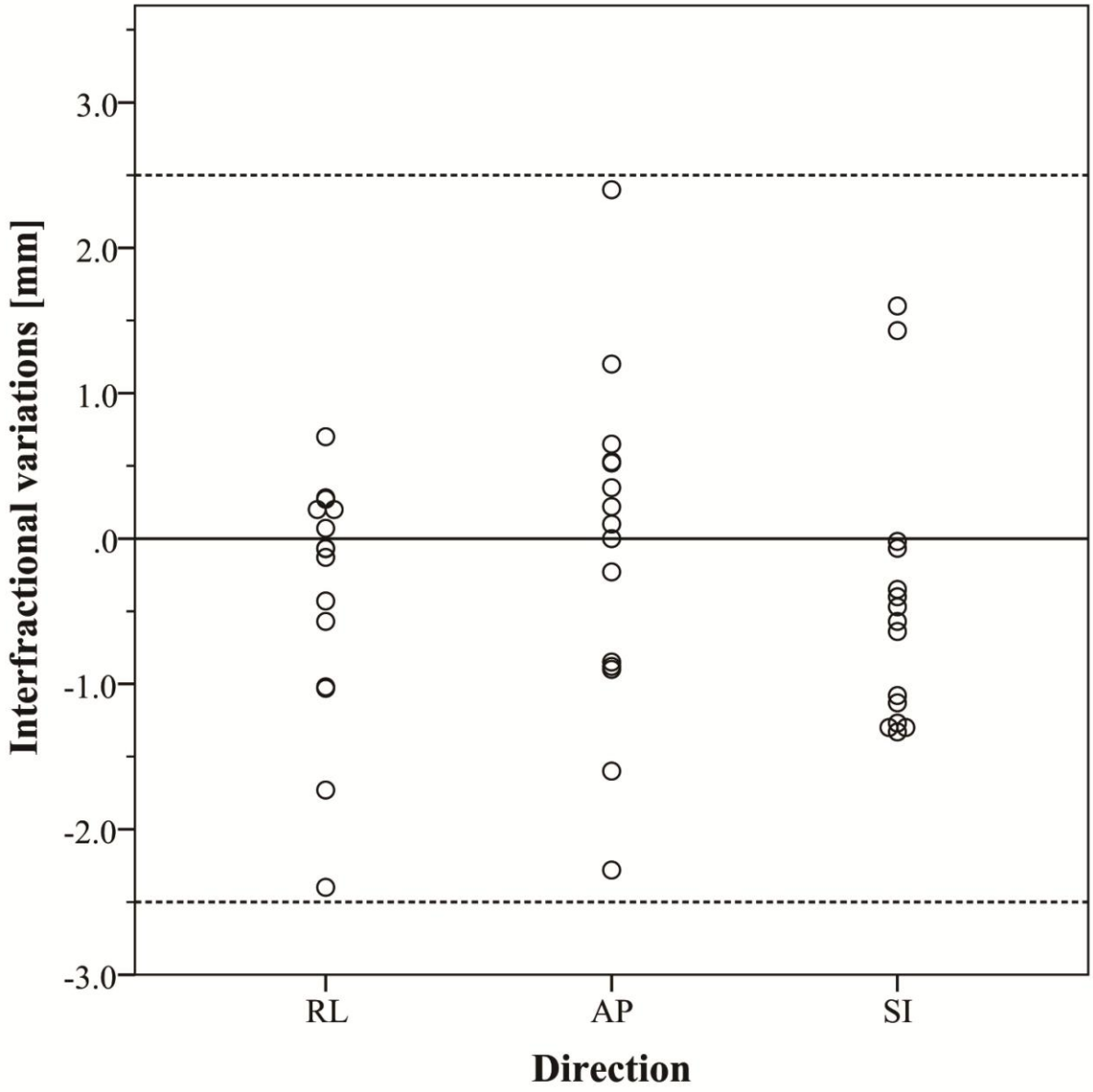
3.0
2.0
1.0
.0
-1.0
-2.0
-3.0
Interfractional variations [mm]
RL
AP
SI
Direction

Fig. 3.